Title
ADDENDEM TO ""QUASIPARTICLE BRANCH MIXING RATES IN SUPERCONDUCTING ALUMINUM""

Author
Chi, C.C.

Publication Date
1979-08-01

Lawrence Berkeley Laboratory
UNIVERSITY OF CALIFORNIA

Materials & Molecular Research Division

Submitted to Physical Review B1

ADDENDEM TO "QUASIPARTICLE BRANCH MIXING RATES IN SUPERCONDUCTING ALUMINUM"

C. C. Chi and John Clarke

August 1979

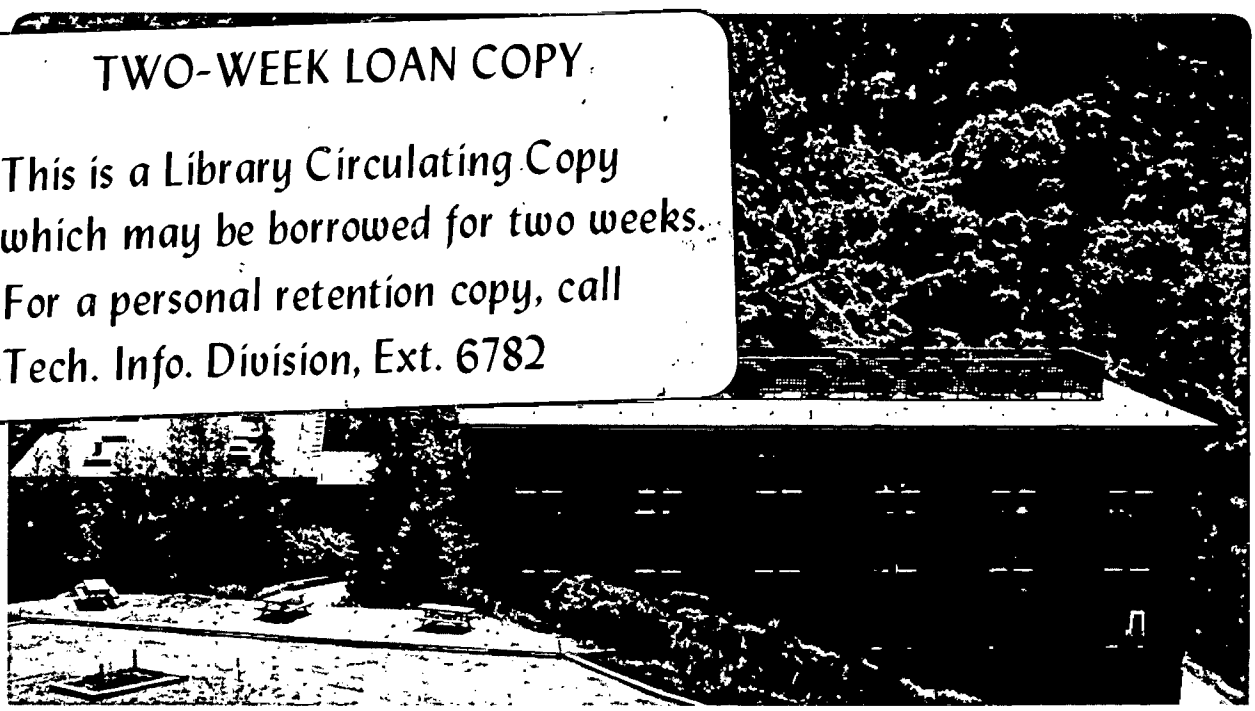

Prepared for the U.S. Department of Energy under Contract W-7405-ENG-48

DISCLAIMER

Addendem to "Quasiparticle Branch Mixing Rates in Superconducting Aluminum"

C. C. Chi* and John Clarke†

Department of Physics, University of California
and Materials and Molecular Research Division
Lawrence Berkeley Laboratory
Berkeley, California 94720

ABSTRACT

The quasiparticle charge distribution generated in a superconductor by tunnel injection from a normal metal is computed as a function of temperature and injection voltage. The low-voltage limiting form is compared with the distributions obtained from the Tinkham-Clarke and Pethick-Smith chemical potential models. The quasiparticle charge relaxation rate $\tau_{Q^*}^{-1}$ due to inelastic scattering is computed for temperatures between $0.3T_c$ and $0.9999T_c$, and for injection voltages between $0.01\Delta(T)/e$ and $20\Delta(T)/e$. The limit $T \rightarrow T_c$ yields the voltage-independent Schmid-Schön and Pethick-Smith result $\tau_{Q^*}^{-1} = \pi\tau_{E=0}^{-1}(T_c)\Delta(T)/4k_BT$, where $\tau_{E=0}^{-1}(T_c)$ is the inelastic scattering rate at the Fermi

energy and at T_c. At temperatures below T_c, both the steady-state distribution function and τ_Q^{-1}* depend on the injection voltage.

I. INTRODUCTION

In a recent paper[1] (CC) we computed the steady-state quasiparticle charge imbalance, Q^*, generated in a superconductor by tunnel injection, together with the charge relaxation rate τ_Q^{*-1}. The purpose of this addendum is to extend the calculations to a much wider temperature range, and to the low-voltage injection limit in which we can compare the results with the predictions of chemical potential models.[2-4]

The steady-state quasiparticle charge imbalance is given by[2,3]

$$Q^* = 2N(0)\int_\Delta^\infty [\delta f_>(E) - \delta f_<(E)]dE, \tag{1}$$

where $N(0)$ is the single spin density of states at the Fermi level, $\delta f_>(E)$ and $\delta f_<(E)$ are the deviations from the equilibrium value $f_T(E)$ for $k>k_F$ and $k<k_F$, and $\Delta(T)$ is the energy gap. CC calculated the relaxation rate for a distribution generated by tunnel injection from a normal metal using

$$\tau_Q^{*-1} = \frac{\dot{Q}^*_{inj}}{Q^*} = \frac{G_{NN}\int_\Delta^\infty \rho_\Delta^{-1}(E)[f(E-eV_{inj}) - f(E+eV_{inj})]dE}{2N(0)e^2\Omega\int_\Delta^\infty [\delta f_>(E) - \delta f_<(E)]dE}, \tag{2}$$

where $\dot{Q}^*_{inj}$ is the generation rate of quasiparticle charge imbalance due to tunnel injection at a voltage V_{inj}, G_{NN} is the tunneling conductance of the injection junction with both materials in the normal state, Ω is the injection volume, and $\rho_\Delta(E) = E/(E^2-\Delta^2)^{1/2}$ is the normalized BCS density of states. The quantities $\delta f_>$ and $\delta f_<$ were computed from

$$\frac{d(\delta f_\varepsilon)}{dt} = G_\varepsilon - G_{in\,\varepsilon} = 0, \tag{3}$$

where $\varepsilon = \pm(E^2-\Delta^2)^{1/2}$ (+ for $k>k_F$, - for $k<k_F$). In Eq. (3),

$$G_\varepsilon = R_o\{\tfrac{1}{2}(1 + \varepsilon/E)[f_T(E-eV_{inj}) - f_T(E)] - \tfrac{1}{2}(1 - \varepsilon/E)[f_T(E) - f_T(E + eV_{inj})]\} \quad (4)$$

is the quasiparticle generation rate due to tunnel injection with $R_o \equiv G_{NN}/2N(0)e^2\Omega$, and

$$\begin{aligned} G_{in\,\varepsilon} = {} & \tau_o^{-1}(k_BT_c)^{-3}\int_{-\infty}^{\infty}d\varepsilon'\Big[\tfrac{1}{2}\Big(1 - \frac{\varepsilon\varepsilon'}{EE'} + \frac{\Delta^2}{EE'}\Big)(E + E')^2 \times \\ & [(f_T(E) + N_T(E + E'))\delta f_{\varepsilon'} + (f_T(E') + N_T(E + E'))\delta f_\varepsilon + \delta f_\varepsilon\delta f_{\varepsilon'}] \\ & + \tfrac{1}{2}\Big(1 + \frac{\varepsilon\varepsilon'}{EE'} - \frac{\Delta^2}{EE'}\Big)(E - E')^2\{\Theta(E - E')[(-f_T(E) - N_T(E - E'))\delta f_{\varepsilon'} \\ & + (1 - f_T(E') + N_T(E - E'))\delta f_\varepsilon - \delta f_\varepsilon\delta f_{\varepsilon'}] \\ & + \Theta(E' - E)[(f_T(E) - N_T(E' - E) - 1)\delta f_{\varepsilon'} + (f_T(E') + N_T(E' - E))\delta f_\varepsilon \\ & + \delta f_\varepsilon\delta f_{\varepsilon'}]\}\Big] \end{aligned} \quad (5)$$

is the inelastic collision integral. In Eq. (5), Θ is the Heaviside function, and $\tau_0^{-1} = 2\pi k_BT_c\alpha^2F(k_BT_c/\hbar)/\hbar$, where α is the matrix element for the electron-phonon interaction, and $F(\omega)$ is the phonon density of states. We assume that α^2F is quadratic in ω. In this addendum we confine our attention to the case of inelastic scattering, and neglect the effects of elastic scattering in the presence of gap anisotropy. Furthermore, we are interested only in the limit $|\delta f_\varepsilon| \ll f_T(E)$, so that terms proportional to $\delta f_\varepsilon\delta f_{\varepsilon'}$ in Eq. (5) can be neglected. It is easy to see from Eqs. (3) to (5) that the steady state solution of δf_ε is proportional to $R_o\tau_o$.

In Fig. 1 of CC, curve *a* shows an example of $(\delta f_> - \delta f_<)/R_o\tau_o$ for $V_{inj} = 10\Delta(T)/e$ and $t = T/T_c = 0.9$. In the same figure, curve *c* shows

the functional form of $(\delta f_> - \delta f_<)_{TC}$ from the Tinkham-Clarke[2,3] (TC) chemical potential model,

$$(\delta f_> - \delta f_<)_{TC} = [-\partial f_T(E)/\partial E](\mu_> - \mu_<), \tag{6}$$

where $\mu_>$ and $\mu_<$ are the chemical potentials for $k>k_F$ and $k<k_F$. Clearly, the agreement is poor, particularly for quasiparticles near the energy gap. Recently, Pethick and Smith[4] (PS) proposed that one should measure ε (rather than E) relative to a single shifted chemical potential, μ, so that $E = [\Delta^2 + (\varepsilon - \delta\mu)^2]^{1/2}$, where $\delta\mu$ is the change of μ relative to the pair electrochemical potential. In this scheme $\delta f = (\partial f_T/\partial E)(\partial E/\partial\mu)\delta\mu = (-\partial f_T/\partial E)(\varepsilon/E)\delta\mu$, so that

$$(\delta f_> - \delta f_<)_{PS} = 2\left(-\frac{\partial f_T}{\partial E}\right)\frac{|\varepsilon|}{E}\,\delta\mu. \tag{7}$$

The use of Eq. (7) rather than Eq. (6) to calculate $\delta f_> - \delta f_<$ will obviously affect the distribution significantly, particularly at energies near the gap. Note that the TC and PS expressions for δf are independent of V_{inj}.

In Sections II and III we compute the distribution function and $\tau_Q^{-1}*$, respectively, for temperatures between $0.3T_c$ and $0.9999T_c$ and for injection voltages between $0.01\Delta(T)$ and $20\Delta(T)$, and compare the results with the predictions of the TC and PS chemical potential models.

II. QUASIPARTICLE DISTRIBUTION FUNCTION

Figure 1 shows $\delta f_> - \delta f_<$ vs. $E/\Delta(T)$ for the low voltage limit, $V_{inj} = 0.01\Delta(T)/e$, and for $t = 0.9$ and 0.99. The solid lines are the computed steady state values, while the dotted and dashed lines are from the TC and PS chemical potential models. The last two curves have

been normalized to represent the same value of Q^* as the first curve. It is immediately obvious that the PS curve is a much better representation of the low-injection voltage steady state distribution than the TC curve, in that it gives the correct location of the peak as well as a very similar general shape. Note that the differences among the three curves become progressively smaller as T approaches T_c. To illustrate the injection voltage dependence, Fig. 2 shows the computed steady-state $\delta f_> - \delta f_<$ for $V_{inj} = 0.01\Delta(T)/e$ (solid curve) and $20\Delta(T)/e$ (dashed curve) at $t = 0.9$ and 0.99. Again, for comparison, the values of δf for both injection voltages are normalized to give the same value of Q^*. Injection at the higher voltage leaves the position of the peak virtually unchanged, but shifts part of the distribution from under the peak into the high energy tail. Figure 2 also shows $\delta f_> + \delta f_<$ for $V_{inj} = 20\Delta(T)/e$, on the same scale as $\delta f_> - \delta f_<$. Low voltage injection does not increase the net quasiparticle population significantly (the curves for $V_{inj} = 0.01\Delta(T)/e$ are indistinguishable from zero on this scale), but high voltage injection increases the magnitude of $\delta f_> + \delta f_<$ substantially relative to $\delta f_> - \delta f_<$. It is noteworthy that at a given value of $E/\Delta(T)$, $(\delta f_> + \delta f_<)/(\delta f_> - \delta f_<)$ decreases as T approaches T_c. This behavior is expected since the ratio should scale roughly as τ_R/τ_Q^*, and the recombination time, τ_R, is roughly constant for $t \geq 0.9$, while τ_Q^* is proportional to $1/\Delta$.

III. VOLTAGE AND TEMPERATURE DEPENDENCE OF τ_Q^{*-1}

In the limit $T \to T_c$, Schmid and Schön[5] and Pethick and Smith[4] have shown that to first order in $\Delta(T)/k_BT$

$$\tau_Q^{*-1} = \pi\tau_{E=0}^{-1}(T_c)\ \Delta(T)/4k_BT, \tag{8}$$

where $\tau_{E=0}^{-1}(T_c)$ is the inelastic scattering rate at T_c and at the Fermi energy. In CC we found that τ_Q^{*-1} computed for $V_{inj} = 10\Delta(T)/e$ and at $t = 0.995$ was about 10% higher than the value given by Eq. (8), suggesting that higher order corrections are important even rather close to T_c. In order to investigate the temperature dependence of τ_Q^{*-1} we have extended our calculations to $0.9999T_c$. Figure 3 shows τ_Q^{*-1} normalized to $\pi\tau_{E=0}^{-1}(T_c)\Delta(T)/4k_BT$ vs. $\Delta(T)/k_BT$ for $t \geq 0.9$ at $eV_{inj} = 0.01\Delta(T)$, $10\Delta(T)$, and $10k_BT_c$. In the low voltage injection limit and for $\Delta(T)/k_BT \leq 0.6$, we find that the computed curve is fitted to within 1% by the empirical formula

$$\tau_Q^{*-1}\tau_{E=0}(T_c)(4/\pi)k_BT/\Delta(T) = 1 + \frac{1}{2}\left(\Delta(T)/k_BT\right) - \frac{3}{4}\left(\Delta(T)/k_BT\right)^2. \tag{9}$$

As the injection voltage is raised, τ_Q^{*-1} increases at all temperatures below T_c. This reflects the increase in the inelastic scattering rate with increasing energy that is also evident in the distribution functions shown in Fig. 2. The 10% increase in τ_Q^{*-1} at $t = 0.995$ and $eV_{inj} = 10\Delta(T)$ noted in CC is clearly demonstrated.

To compare these results with the predictions of the TC and PS chemical potential models, we have used the following scheme to compute τ_Q^{*-1} from the TC and PS distributions:

(i) The appropriate distribution function [Eq. (6) or (7)] is used for δf_ε in Eq. (5) to obtain $G_{in\ \varepsilon}$.

(ii) The values of $G_{in\ \varepsilon}$ are used in Eq. (3) to obtain the injection rate G_ε.

(iii) The values of G_ε are used to calculate $\dot{Q}^*_{inj}$ from $\dot{Q}^*_{inj} = \int_o^\infty d\varepsilon(\varepsilon/E)(G_\varepsilon - G_{-\varepsilon})$.

(iv) The ratio of $\dot{Q}^*_{inj}/Q^*$ yields $\tau_Q^{-1}{}^*$ [Eq. (2)].

The dotted and dashed lines in Fig. 3 represent the results for the TC and PS models.[6] We note that the TC curve is surprizingly close to the low-voltage computed curve, while the PS curve lies significantly higher except at temperatures exceedingly close to T_c. These results can be understood qualitatively by inspection of the distributions shown in Fig. 1. Although the PS distribution is a good representation of the computed steady state distribution, it contains less quasiparticle charge near the peak and more at high energies than the computed distribution. Since the quasiparticle charge relaxation rate increases monotonically with energy, the PS distribution leads to a higher overall relaxation rate than the low voltage limit. On the other hand, the TC distribution intersects the low-voltage distribution at two points, and lies very close to it except at energies near the gap. As a result, the average charge relaxation rates for the two distributions turn out to be almost identical. Thus, the good agreement in $\tau_Q^{-1}{}^*$ between the computed low-voltage curve and the TC curve appears to be accidental.

The temperature dependence of $\tau_Q^{-1}*$, normalized to $\pi\tau_{E=0}^{-1}(T_c)/4$, is shown in Fig. 4 for temperatures down to 0.3 T_c. Curves are shown for $\tau_Q^{-1}*$ determined from the computed steady state distribution at $eV_{inj} = 0.01\Delta(T)$ and $10\Delta(T)$, and from the PS distribution. As the temperature is lowered from T_c, $\tau_Q^{-1}*$ goes through a peak at an injection-voltage dependent temperature between 0.8 and $0.9T_c$, and then decreases steadily. As in Fig. 3, the PS curve always lies above the low-voltage curve. It should be emphasized that these curves are computed only for inelastic scattering processes, and that in real superconductors elastic scattering in the presence of an anisotropic energy gap is likely to increase the low temperature charge relaxation rate very substantially.[1-3]

Finally, Fig. 5 shows $\tau_Q^{-1}*$ and $(F^*\tau_Q*)^{-1}$, normalized to $\pi\tau_{E=0}^{-1}(T_c)\Delta(T)/4k_BT$, vs. $eV_{inj}/\Delta(T)$ at $t = 0.9$, where $F^* = e\Omega Q_{inj}^*/I_{inj}$, and I_{inj} is the injection current. The experimentally measured voltage, V_d, is thus directly proportional to $(F^*\tau_Q*)I_{inj}$[1]. We see that for $V_{inj} \gtrsim 6\Delta(T)/e$ the voltage dependences of τ_Q* and F^* cancel,[7] so that $F^*\tau_Q*$ becomes independent of voltage, and V_d becomes linear in I_{inj}, as is observed experimentally.[1]

ACKNOWLEDGMENTS

We are grateful to Professor M. Tinkham who pointed out to us the close agreement between our computed low-voltage distribution and the PS distribution. We thank Professors C. J. Pethick and H. Smith for useful discussions and the communication of their variational calculations of $\tau_Q^{-1}*$, and to Dr. T. Lemberger for many helpful conversations and a critical reading of the manuscript. This work was supported by the Division of Materials Sciences, Office of Basic Energy Sciences, U. S. Department of Energy.

REFERENCES

*Current address: IBM Thomas J. Watson Research Center, P. O. Box 218, Yorktown Heights, New York, 10598.

†Guggenheim Fellow.

1. C. C. Chi and J. Clarke, Phys. Rev. B19, 4495 (1979).

2. M. Tinkham and J. Clarke, Phys. Rev. Lett. 28, 1366 (1972).

3. M. Tinkham, Phys. Rev. B6, 1747 (1972).

4. C. J. Pethick and H. Smith, to be published in Ann. of Phys. (1979).

5. A. Schmid and G. Schön, J. Low Temp. Phys. 20, 207 (1975).

6. C. J. Pethick and H. Smith (private communication) have used a variational calculation with their chemical potential model to obtain a curve identical with that shown for their model in Fig. 3.

7. For $V_{inj} >> \Delta(T)/e$, $F^* \approx 1 - \pi\Delta(T)/2eV_{inj}$ [CC, Eq. (2.11)]. Unfortunately, owing to a drafting error, the plot of F^* vs. $\Delta(T)/k_BT$ for $V_{inj} = 10\Delta(T)/e$ in the inset of Fig. 2 of CC shows an incorrect limiting value of about 0.87 for $\Delta(T)/k_BT_c \gtrsim 0.5$. The correct limiting value should be about 0.84, as given by Eq. (2.11) of CC.

FIGURE CAPTIONS

Fig. 1 $\delta f_>(E) - \delta f_<(E)$ vs. $E/\Delta(T)$ at (a) $t = 0.9$ and (b) $t = 0.99$: ——— steady state calculation with $V = 0.01\Delta(T)/e$, ... TC chemical potential model, and - - - - - - PS chemical potential model.

Fig. 2 Steady state calculations of $\delta f_>(E) - \delta f_<(E)$ and $\delta f_>(E) + \delta f_<(E)$ vs. $E/\Delta(T)$ at (a) $t = 0.9$ and (b) $t = 0.99$: ——— $V = 0.01\Delta(T)/e$, and - - - - - - $V = 20\Delta(T)/e$.

Fig. 3 $4\tau_Q^{*-1}\tau_{E=0}(T_c)k_BT/\pi\Delta(T)$ vs. $\Delta(T)/k_BT$ and T/T_c. Steady state calculation for $eV_{inj} = 0.01\Delta(T)$ (— □ —), $10\Delta(T)$ (— o —), and $10k_BT_c$ (— Δ —); TC model (. . . . .), and PS model (- - - - -).

Fig. 4 $4\tau_Q^{*-1}\tau_{E=0}(T_c)/\pi$ vs. $\Delta(T)/k_BT$ and T/T_c. Steady state calculation for $eV_{inj} = 0.01\Delta(T)$ (— □ —) and $10\Delta(T)$ (— o —); PS model (- - - - -).

Fig. 5 $4\tau_Q^{*-1}\tau_{E=0}(T_c)k_BT/\pi\Delta(T)$ and $4(F^*\tau_Q^*)^{-1}\tau_{E=0}(T_c)k_BT/\pi\Delta(T)$ vs. $eV_{inj}/\Delta(T)$.

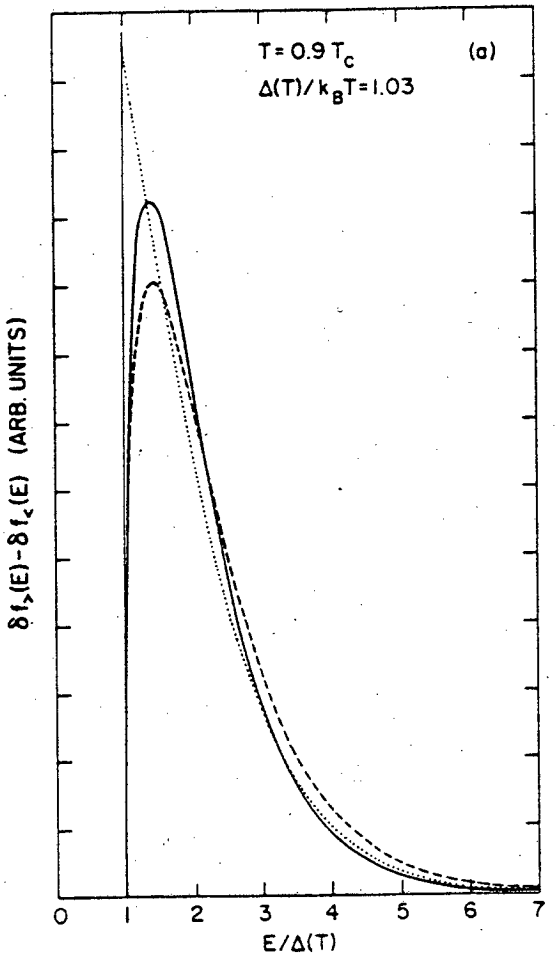
T = 0.9 T_c
(a)
Δ(T)/k_B T = 1.03
δf_>(E) - δf_<(E) (ARB. UNITS)
0
1
2
3
4
5
6
7
E/Δ(T)

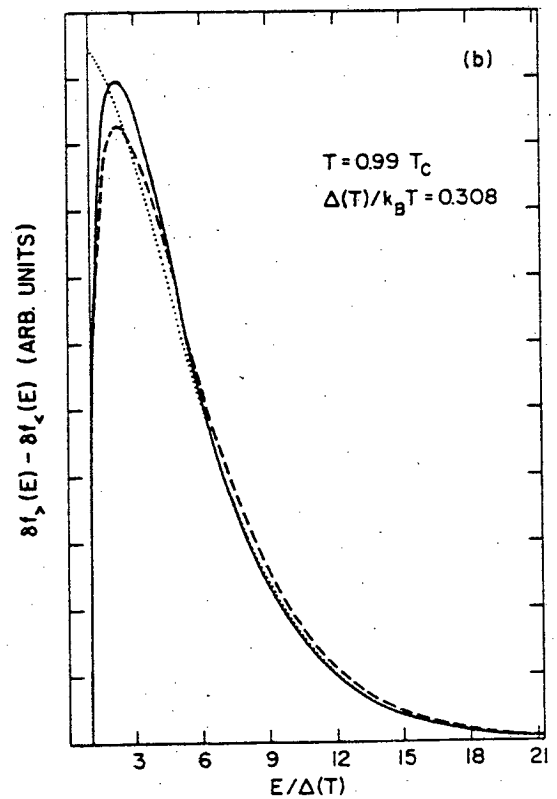
(b)
T = 0.99 T_c
Δ(T)/k_B T = 0.308
δf_>(E) - δf_<(E) (ARB. UNITS)
3
6
9
12
15
18
21
E/Δ(T)

Figure 1

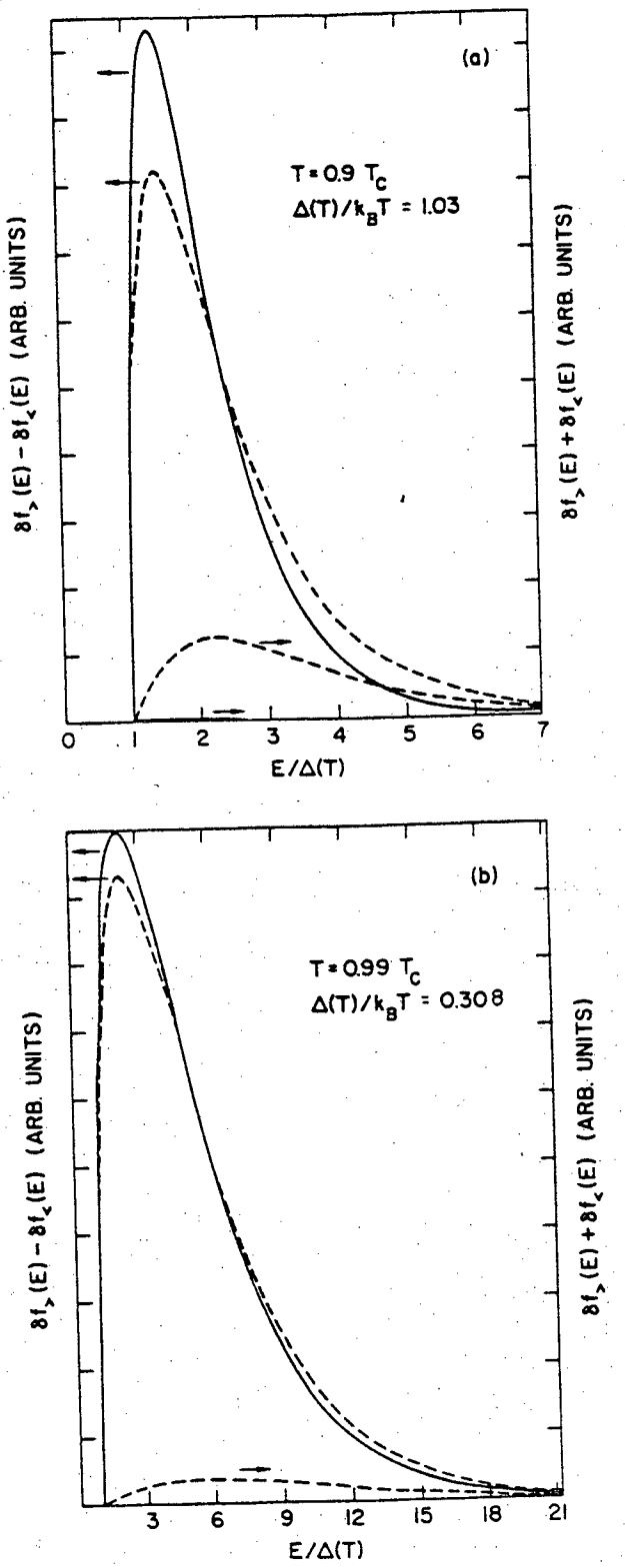
(a)
T = 0.9 T_c
Δ(T)/k_BT = 1.03
δf_>(E) − δf_<(E) (ARB. UNITS)
δf_>(E) + δf_<(E) (ARB. UNITS)
0
1
2
3
4
5
6
7
E/Δ(T)
(b)
T = 0.99 T_c
Δ(T)/k_BT = 0.308
δf_>(E) − δf_<(E) (ARB. UNITS)
δf_>(E) + δf_<(E) (ARB. UNITS)
3
6
9
12
15
18
21
E/Δ(T)

Figure 2

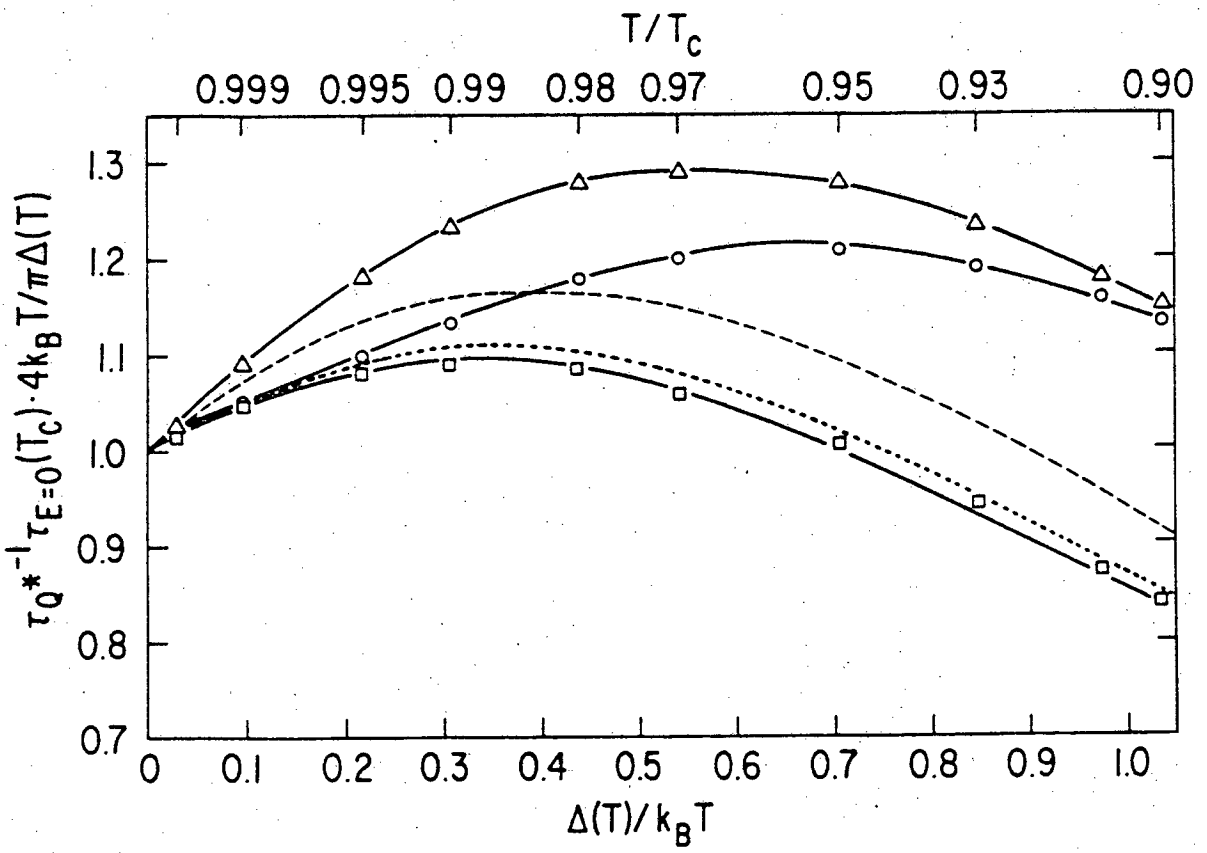
T/T_c
0.999 0.995 0.99 0.98 0.97 0.95 0.93 0.90
τ_Q*^-1 τ_E=0(T_c)·4k_B T/πΔ(T)
1.3
1.2
1.1
1.0
0.9
0.8
0.7
0 0.1 0.2 0.3 0.4 0.5 0.6 0.7 0.8 0.9 1.0
Δ(T)/k_B T

Figure 3

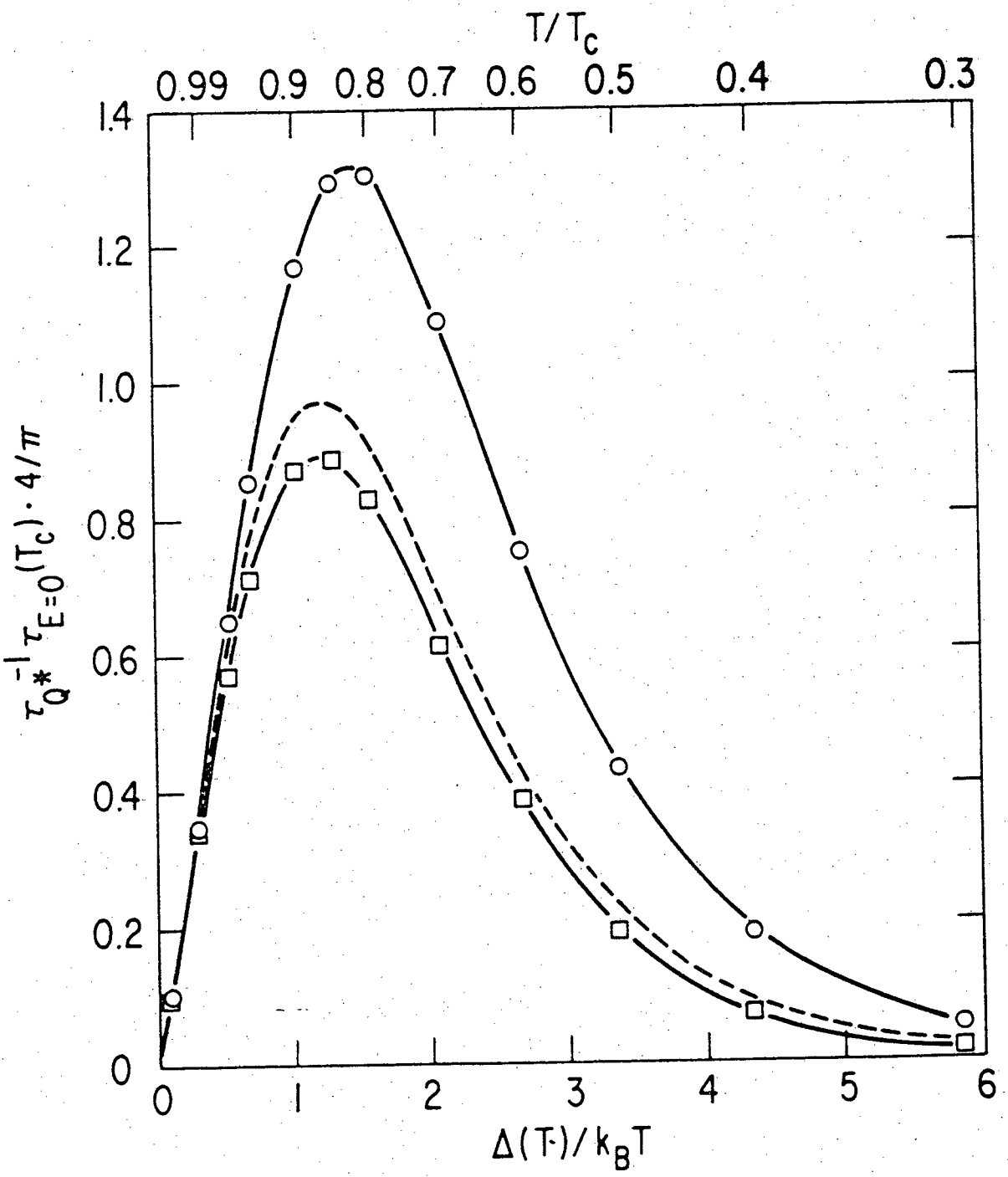
T/T_c
0.99 0.9 0.8 0.7 0.6 0.5 0.4 0.3
1.4
1.2
1.0
0.8
0.6
0.4
0.2
0
τ_Q*^-1 τ_E=0(T_c) · 4/π
0 1 2 3 4 5 6
Δ(T)/k_BT

Figure 4

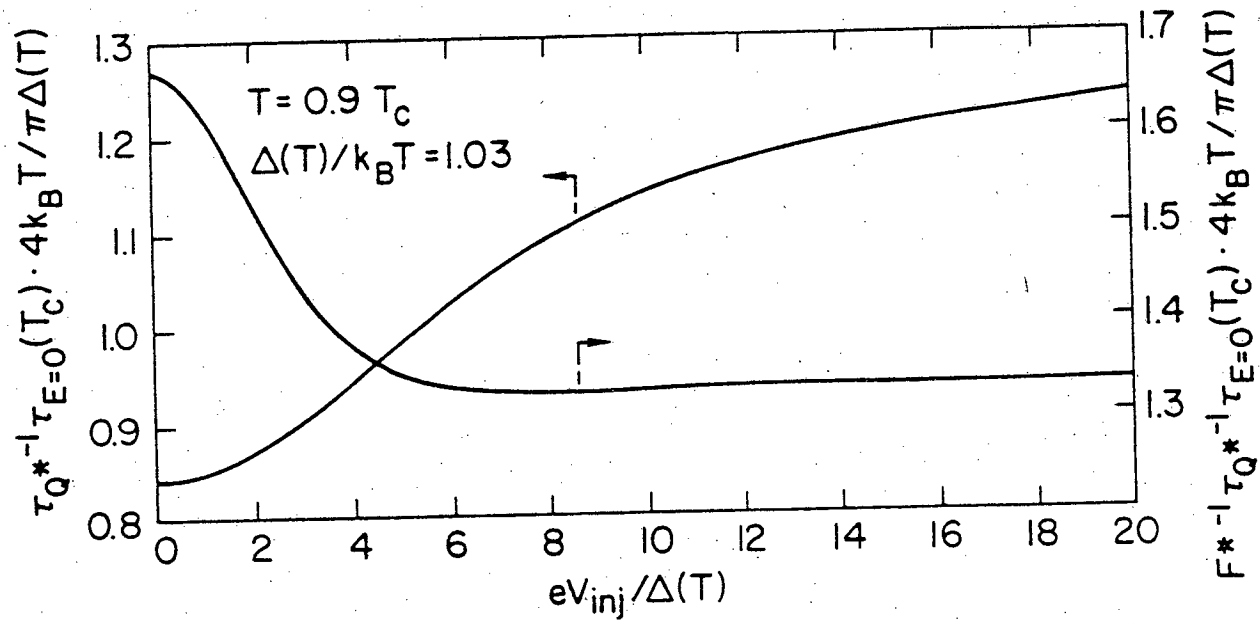
T = 0.9 T_c
Δ(T)/k_BT = 1.03
τ_Q*^-1 τ_E=0(T_c) · 4k_BT/πΔ(T)
F*^-1 τ_Q*^-1 τ_E=0(T_c) · 4k_BT/πΔ(T)
eV_inj/Δ(T)
0.8
0.9
1.0
1.1
1.2
1.3
1.3
1.4
1.5
1.6
1.7
0
2
4
6
8
10
12
14
16
18
20

Figure 5

This report was done with support from the Department of Energy. Any conclusions or opinions expressed in this report represent solely those of the author(s) and not necessarily those of The Regents of the University of California, the Lawrence Berkeley Laboratory or the Department of Energy.

TECHNICAL INFORMATION DEPARTMENT
LAWRENCE BERKELEY LABORATORY
UNIVERSITY OF CALIFORNIA
BERKELEY, CALIFORNIA 94720